POLITECNICO DI TORINO
Repository ISTITUZIONALE

Silver-functionalized polyvinyl alcohol nanofiber membranes: A comparative study of nanoparticle incorporation and coating deposition

Original
Silver-functionalized polyvinyl alcohol nanofiber membranes: A comparative study of nanoparticle incorporation and coating deposition / Gattucci, F., Rossi, M., Sarchini, L., Bertarelli, C., Castagna, R., Balagna, C.. - In: SURFACE & COATINGS TECHNOLOGY. - ISSN 0257-8972. - 520:(2026), pp. 1-10. [10.1016/j.surfcoat.2025.133038]

Availability:
This version is available at: 11583/3005728 since: 2025-12-09T10:18:33Z

Publisher:
Elsevier

Published
DOI:10.1016/j.surfcoat.2025.133038

Terms of use:

This article is made available under terms and conditions as specified in the corresponding bibliographic description in the repository

Publisher copyright

(Article begins on next page)

26 November 2026

Surface & Coatings Technology 520 (2026) 133038

Contents lists available at ScienceDirect

Surface & Coatings Technology

journal homepage: www.elsevier.com/locate/surfcoat

Silver-functionalized polyvinyl alcohol nanofiber membranes: A comparative study of nanoparticle incorporation and coating deposition

Francesca Gattucci [a,1], Martina Rossi [b,1], Letizia Sarchini [b], Chiara Bertarelli [b], Rossella Castagna [b], Cristina Balagna [a,*]

[a] Department of Applied Science and Technology, Politecnico di Torino, Corso Duca degli Abruzzi 24, 10129, Turin, Italy
[b] Dipartimento di Chimica Materiali e Ingegneria Chimica Giulio Natta Politecnico di Milano Piazza Leonardo da Vinci 32, Milano, 20133, Italy

ARTICLE INFO

Keywords:
PVA
Silver nanoparticles AgNPs
Electrospinning
PVD
Antibacterial
Coating

ABSTRACT

Preventing contact with pathogens is a critical requirement in filtration applications for both public and private environments. Developing antibacterial membranes is essential to enhance protection and mitigate contamination risks. In this work, a direct comparative study of two silver-based functionalization strategies applied to electrospun polyvinyl alcohol (PVA) nanofiber membranes is presented, aiming to identify the most effective approach for producing durable antibacterial filters. The first method involves in-fiber incorporation of silver nanoparticles (AgNPs) by electrospinning a colloidal AgNP dispersion blended with the PVA solution, followed by crosslinking. The second method uses physical vapor deposition (PVD) to deposit a silica- or zirconia-based composite coating embedding silver nanoclusters onto pre-crosslinked PVA fibers. Both types of membranes were characterized at each processing stage. Morphological changes were assessed by FESEM and image analysis, surface wettability by contact angle measurements, and silver content by EDS. Antibacterial activity was tested against both Gram-positive and Gram-negative bacteria, while silver ion release in water was monitored to evaluate the ability of the inorganic matrix to control Ag^{+} leaching.

The results show that, although both strategies confer antibacterial properties, the PVD-based coating provides a more uniform silver surface distribution, controlled and sustained silver release, and preservation of nanofiber morphology, making it a promising route for the fabrication of high-performance antibacterial membranes.

1. Introduction

Bacterial contamination can be a vehicle for infections transmission, and it represents a substantial risk to public health [1]. Bacterial infections are usually treated with antibiotics, but their overuse over the years has led to the emerging problem of multidrug resistance in bacteria, which the World Health Organization (WHO) has identified as a serious global health threat [2]. Treating infections, in fact, is becoming increasingly difficult, making the prevention of contact with contaminants the primary goal in order to avoid infection.

In this context, reducing the presence of microbial contaminants in the environment has become a key strategy to protect public health. Decontaminating water and air is crucial in both hospitals and public spaces [3]. Contaminated water may contain bacteria, viruses, protozoa, and parasites that can cause waterborne diseases, which can be life-threatening, particularly for immunocompromised individuals; this issue is not limited to developing countries as outbreaks of contaminated water in developed nations also present serious public health risks and economic costs [4]. Infections can also be transmitted through the air, typically through the spread of droplets containing pathogens [5]. To mitigate the spread of airborne diseases, the World Health Organization recommends the use of ventilation systems, air purification technologies, and personal protective equipment such as masks and respirators [6]. Several studies have highlighted the critical role of airborne infection transmission in healthcare environments [7]. Additionally, air pollution from particulate matter (PM) contributes to health issues such as skin irritation, asthma and, in the worst cases, cancer [8]. PM can interact with bacteria, enhancing bacterial proliferation and biofilm formation [9]. In addition, volatile organic compounds (VOCs) are harmful pollutants that can increase the risk of respiratory illnesses, compounding the impact of bacterial infections [10].

Given the significant health risks posed by airborne and waterborne

* Corresponding author.
E-mail address: cristina.balagna@polito.it (C. Balagna).
[1] These authors contributed equally to this work.

https://doi.org/10.1016/j.surfcoat.2025.133038
Received 15 August 2025; Received in revised form 20 November 2025; Accepted 3 December 2025
Available online 6 December 2025
0257-8972/© 2025 The Author(s). Published by Elsevier B.V. This is an open access article under the CC BY-NC-ND license (http://creativecommons.org/licenses/by-nc-nd/4.0/).

contaminants, including particulate matter, bacteria, and VOCs, effective decontamination strategies are essential. Absorption and filtration techniques are widely used for water and air decontamination [4]. Fibrous filters are often employed to remove solid particles from air streams because of their simplicity and low cost, and electrospun fibers, have gained attention for their high surface area and porosity [11]. However, the use of filters has limitations. Materials can become saturated with microbes, leading to biofilm formation that enables bacteria to survive and become a persistent source of pathogens, posing a particular risk to immunocompromised individuals [12]. To prevent bacterial growth, antibacterial filters are recommended.

One of the leading fabrication methods for filtering membranes is electrospinning, a versatile technique to produce continuous polymer nanofibers. This method yields fibers with unique properties such as high surface-to-volume ratio, tunable porosity and uniform diameter [13,14]. The electrospinning process is essentially based on the accumulation of charges on the surface of a polymer solution flowing from a needle tip under a high-voltage electric field, which leads to the formation and ejection of a charged jet. The strong electric field applied between the syringe needle and the collector rapidly stretches the flying jet, whose behavior is strongly influenced by the rheological properties of the feed solution [15]. During its flight, the polymer jet undergoes thinning due to electrostatic repulsion and solvent evaporation, resulting in a gradual reduction in diameter [16] and the formation of continuous fibers.

Thanks to the properties provided by their nanostructure, fibers and membranes produced through electrospinning can be used in various fields such as sensing [17], optoelectronics [18], chemical filtration [19,20], and biomedical applications [21].

For filtration, the use of nanofibers offers significant advantages over traditional filters as they combine high filtration efficiency with a low pressure drop [22]. The reduced diameter and high surface area of electrospun substrates enable a slip flow regime, making them suitable for high-efficiency filters, breathable protective clothing, and face masks. Furthermore, in air and water purification systems, the high surface area and porosity of electrospun fibers facilitate the effective interaction of antibacterial agents with contaminants, enhancing their antimicrobial effectiveness without compromising membrane permeability [23].

Ultimately, post-processing treatments can expand the range of applications of these membranes by modifying their chemical and physiochemical properties through surface functionalization [24], heat treatments, physical sputtering deposition of inorganic materials, crosslinking and immobilization of biological components [20], hydrolysis and oxidation [25].

Among dry approaches, plasma treatment and sputtered coating deposition are commonly used [26]. Sputtering is particularly advantageous for modifying thermosensitive materials, such as natural fibers or polymers, as it avoids the use of toxic chemicals and does not produce waste [27].

In addition, sputtering has become a versatile method for modifying and functionalizing materials, including electrospun fibers, due to the high uniformity of the deposited coatings [28]. Conductive surfaces have been created by functionalizing thin polyamide fibers through sputter deposition of copper [29] and by coating polyamide (PA6) fibers with gold and palladium [26]. For antibacterial applications, silver nanocoatings have been deposited on polysulfone (PSU) electrospun membranes [30]; however, some coatings show rapid release of antibacterial agents when not embedded in a matrix [31]. Coatings containing antibacterial agents can act as reservoirs, facilitating localized release and improving the efficiency of antibacterial action [32]. Ferraris et al. [33–35] patented an antimicrobial/antiviral coating composed of silver nanoclusters embedded in a ceramic or glass matrix. This coating, created through co-sputtering, showed excellent antimicrobial and antiviral performance [27,33,34,36–39].

Polyvinyl alcohol (PVA) was selected due to its excellent electrospinnability which ensure the formation of nanometric fibers, thereby providing a large exchange surface for filtration. Moreover, PVA can be electrospun from aqueous solutions, thereby avoiding the use of harmful organic solvents [14].

However, this water processability also results in the water solubility of the resulting fibers, leading to rapid degradation upon exposure to aqueous environments. Although this property may be attractive for biomedical applications and controlled drug delivery, the use of such fibers as air and water filters requires the crosslinking of the membrane to improve its stability and maintain structural integrity in humid or liquid media [20].

To exert an antimicrobial effect, nanofibers serve as the optimal substrate for functionalization with antimicrobial agents due to their high exposed surface area. The large surface area provided by the nanostructure results in a higher efficiency owing to the increased exposure of the surface to microorganisms, leading to improved antimicrobial activity [23,40].

It is well known that silver-based compounds exhibit a strong inhibitory and bactericidal effect, along with a broad spectrum of antimicrobial activity against bacteria, fungi, and viruses [41,42].

Among all silver-based compounds, silver nanoparticles (AgNPs) are widely used in the fields of air and water purification, biomedical, textiles, and wound dressings [23,40]. Therefore, nanoparticles have been selected as the antibacterial agent in the present study; in particular, they have been integrated into the electrospun fibers according to two different methodologies i) blending AgNPs with the PVA solution and electrospinning and ii) depositing AgNPs-containing coatings onto the surface of the electrospun membrane through a post-processing functionalization step.

As a first strategy, the nanoparticle colloidal solution was blended into the polymer solution prior to electrospinning. This method has been explored in many studies for antibacterial application [43] and for the fabrication of SERS sensitive surfaces [44] and it leads to the successful one-pot production of PVA-AgNPs nanofibers forming a fibrous mat. As a second strategy, the electrospun membrane was subjected to a post-functionalization process to decorate the fiber surface with AgNPs. A patented sputtered coating [35] of a silica or zirconia matrix embedding AgNPs was deposited onto the electrospun membrane. This layer is known for its strong antibacterial properties but has never been applied to electrospun fibers to produce antibacterial membranes before.

Several studies have explored the use of PVD techniques to functionalize in the post-process electrospun nanofibers with inorganic and in particular metallic coatings, demonstrating that thin conformal layers can be deposited without compromising the nanofiber morphology kadavil valerini maliszewska [45–47]. Other works have reported the incorporation of silver nanoparticles (AgNPs) into electrospun fibers by blending them directly into the polymer solution prior to electrospinning, achieving a one-pot antimicrobial functionalization meng lee [48,49].

However, despite the growing interest in both approaches, no previous study has directly compared AgNP incorporation within Poly (vinyl alcohol) (PVA) fibers and PVD-deposited Ag-containing coatings on electrospun membranes under the same processing and testing conditions.

In this study, such a comparison is presented, evaluating in-fiber AgNP incorporation and PVD-deposited coatings in terms of structure, silver release control, and antimicrobial efficiency, mainly for filtration applications.

2. Materials and methods

2.1. Materials

Poly(vinyl alcohol) > 99 % hydrolyzed (PVA) with an average molecular weight of 89,000–98,000 Da, sodium citrate tribasic dihydrate, silver nitrate, sodium borohydride, 50 % aqueous glutaraldehyde (GA),

acetone (≥ 99,5 %) and hydrochloric acid (min. 37 %, HCl) were purchased from Sigma Aldrich. All chemicals and solvents were used as received.

2.2. Preparation of electrospun PVA membrane

2.2.1. Preparation of PVA solution

The weighed PVA powder was dissolved directly in water with a concentration of 12 % *w*/w. The solution was stirred at 95 °C for 1 h then slowly cooled down to room temperature in order to obtain a clear solution without precipitates.

2.2.2. Electrospinning of PVA membranes

The electrospinning process was carried out using a horizontal setup, in particular the system included an infusion pump (KDS Scientific, model series 200) holding a syringe (Hamilton Gastight model 1002 TLL) equipped with a 22-gauge needle. A high-voltage power supply (Spellman SL30P30) was connected to the system allowing the formation of a potential difference between the needle of the syringe and the static collector.

Initially, samples were deposited on a glass substrate attached to the collector with copper tape for preliminary inspection under an optical microscope. This preliminary analysis was carried out in order to detect the possible presence of beads or inhomogeneities in fiber morphology. Subsequently, samples were deposited onto silicon substrates for the detailed characterizations.

The process was carried out at room temperature (20 °C and 23 °C), which did not have a significant effect on the process. Conversely, it was noticed that the relative humidity varying between days (ranging from 25 % to 40 %), played a relevant role on the spinnability. Electrospinning of PVA at high relative humidity values has been avoided since it led to defective fibers under all the experimental condition tested.

Keeping the distance between the collector and the needle constant at 20 cm and varying the other parameters, PVA fibers with different morphologies were obtained. In particular, the optimal electrospinning parameters were found to be a flow rate of 0.2 mL/h with an applied voltage of 14 kV. Afterwards, the fibers were deposited using the above parameters onto 1 cm × 1 cm glass substrates for 2 h until a thick and homogeneous mat was obtained.

2.3. Chemical cross-linking of electrospun mats

The chemical crosslinking was performed according to the previous study by *Castagna* et al. [20], with a modified immersion time. All the electrospun mats were immersed in a 0.15 M glutaraldehyde in acetone-water solution bath with 0.05 M HCl for 40 min. Afterwards, the samples were washed in distilled water for 1 h to remove any excess crosslinker possibly adsorbed on the fiber surface and dried by gentle solvent evaporation for several hours.

2.4. Silver functionalization of electrospun PVA membrane

2.4.1. Silver nanoparticles synthesis

All glass substrates were cleaned with nitric acid, rinsed with distilled water, and dried before further use. This procedure prevents the presence of contaminants that could affect the nucleation of nanoparticles. For the preparation of silver nanoparticles 10 mL of 0.034 M sodium citrate aqueous solution and 37 mL of distilled water were added inside to a round-bottom flask with reflux, and the mixture was heated to 70 °C for 15 min, the temperature was monitored using a thermometer. Afterwards 0.9 mL of 0.06 M silver nitrate ($AgNO_3$) aqueous solution was added to the mixture, followed by 1 mL of 0.026 M sodium borohydride ($NaBH_4$) aqueous solution quickly added. The solution was kept at 70 °C under vigorous stirring for 1 h and then cooled to room temperature.

2.4.2. Preparation of PVA-AgNPs solution

The concentration of the nanoparticles was increased by centrifugation for 20 min at 17000 rpm. Upon the removal of the supernatant, the volume was reduced from 100 mL to 2.5 mL.

PVA powder was dissolved directly in the colloidal solution at a polymer/solvent (containing the silver nanoparticles) concentration of 12 % *w*/w. The solution was mixed using a magnetic stirrer at 95 °C for 1 h until a uniform solution was obtained.

2.4.3. Preparation of PVA-AgNPs membranes

After a preliminary analysis, the optimal electrospinning parameters were found to be a collector to tip distance of 25 cm, flow rate of 0.05 mL/h, applied voltage of 18 kV. Afterwards, the fibers were deposited according to the above parameters onto 1 × 1 cm^2 glass substrates for 16 h until a thick and homogeneous mat was obtained. After these steps the produced membranes were crosslinked using the previously mentioned method.

2.4.4. Co-sputtered coating deposition on electrospun and crosslinked PVA membrane

The composite coatings were applied onto the crosslinked PVA membranes and consisted of silver nanoclusters embedded within a silica or zirconia matrix, deposited using a patented co-sputtering technique [35] onto the PVA electrospun and crosslinked membranes. The sputtering apparatus was configured with two targets for each deposition: for the silica-based coating, a silica target (Sigma-Aldrich, 99.99 % purity) and a silver target (Franco Corradi S.r.l., 99.9 % purity); for the zirconia-based coating, a zirconia target (99.98 % ZrO_2, Nanovision™) and the same silver target. The applied powers were as follows depending on the used matrix: for the silica-based coating, 200 W in radio frequency (RF) mode was applied to the silica target, and 5 W in direct current (DC) mode to the silver target; for the zirconia-based coating, 250 W in RF mode was applied to the zirconia target, and 4 W in DC mode to the silver target. All depositions were carried out for 30 min in a pure argon atmosphere at a pressure of 5.5 dPa. The deposition parameters were selected based on previous studies [38,50–52]. The coated membranes were named in the text PVA-SiO_2Ag and PVA-ZrO_2Ag.

2.5. Chemical-physical characterization of the PVA membranes

The as-spun membranes, both before and after crosslinking, as well as those functionalized with silver nanoparticles (AgNPs) and coated via co-sputtering, were characterized and compared. Morphological analyses were carried out using a field emission scanning electron microscope (FESEM, QUANTA INSPECT 200, Zeiss SUPRA 40) at various magnifications to assess the surface morphology of the electrospun fibers, confirm the uniformity and quality of the coatings, and verify the successful electrospinning of silver nanoparticle-functionalized fibers. Observations were made using an in-lens secondary electron detector. Fiber diameter analysis and cluster-size analysis were conducted by measuring 100 fibers from FESEM images using ImageJ software. A Matlab-based script was used to estimate the Root-Mean-Square (RMS) roughness from FESEM images before and after coating (See Supporting Supplementary Information Table S1, Fig. S1). Additionally, AgNPs were characterized by UV–vis spectroscopy (Cary 5000) and by dimensional analysis of FESEM images. Compositional analyses were carried out using energy dispersive spectroscopy (EDS, EDAXPV 9900TM) to determine the atomic percentages of silver in the functionalized fibers.

2.6. Water contact angle

Surface wettability was evaluated by measuring the static water contact angle (WCA) using the sessile drop technique. For each sample, three measurements were performed, and the contact angle was

automatically recorded 2 s after droplet deposition. Results are presented as the mean ± standard deviation (SD).

2.7. Leaching test in water

Following the procedure described in [27], the silver content in the PVA samples containing AgNPs and in those coated by co-sputtering was quantified using Inductively Coupled Plasma Mass Spectrometry (ICP–MS, Agilent Technologies 7700). Each sample (1 × 1 cm^2) was immersed in 5 mL of nitric acid and heated for 30 min. The resulting solution was then diluted with distilled water to a final volume of 25 mL for analysis. The release of silver into water from both the functionalized and coated PVA fibers was assessed through a leaching test performed in Milli-Q water at room temperature. Electrospun fiber samples (1 × 1 cm^2) were immersed in 30 mL of water, with coated samples positioned so that the coated surface faced upward. The water was analyzed after 1 h, 3 h, and 1, 3, 7, and 14 days using a spectrophotometer (Hanna Instruments) to determine the silver ion concentration in parts per million (ppm). All measurements were performed in triplicate to ensure accuracy.

2.8. Antibacterial activity evaluation

The preliminary antibacterial efficacy of the AgNPs functionalized and co-sputtered membranes was evaluated using the qualitative inhibition zone test, following the NCCLS M2-A9 performance standard [53]. Non-pathogenic strains of *Staphylococcus epidermidis* (Gram-positive, ATCC14990) and *Escherichia Coli* (Gram-negative, ATCC8739) were selected as Gram-positive and Gram-negative bacteria, respectively. Bacterial suspensions, adjusted to a McFarland index of 0.5, were spread onto Mueller Hinton agar plates. The AgNPs-functionalized and co-sputtered PVA membranes were then placed on the agar and incubated at 35 °C for 24 h. After incubation, the inhibition zones (halos) surrounding the samples were observed and measured. The samples were further incubated for an additional 24 h to assess the stability of the inhibition zones. The bare PVA membranes were also tested as controls.

3. Results and discussion

3.1. Chemical-physical characterization of the membranes

Fig. 1 shows the morphology of the PVA fibers, both before and after crosslinking. Randomly collected PVA fibers, as electrospun (Fig. 1a,b), are homogeneous, free of any defects or porosity. The associated diameter distribution is well defined and narrow, namely the fibers have a mean diameter of 304 ± 54 nm. After crosslinking (Fig. 1c,d) the fibers do not show any defects, and the mean diameter remains almost unchanged at 317 ± 104 nm.

PVA-AgNPs fibers (Fig. 2), obtained by direct electrospinning of the polymeric solution containing AgNPs, exhibit a uniform morphology without defects. After crosslinking, the fiber morphology remained unchanged (Fig. 2b). Fig. 2c shows a region of the fiber at high magnification where AgNPs are well visible on the surface of the fiber, confirming the successful functionalization.

From the images, an analysis of the diameter distribution is shown in the graph in Fig. SI-1. PVA-AgNPs fibers are characterized by a narrow diameter distribution (332 ± 52 nm). Notably, the addition of silver nanoparticles did not significantly alter the average diameter of the PVA nanofibers, likely due to the inherent polarity of the PVA solution [54]. The crosslinking process does not change the morphology of the fibers (mean diameter = 352 ± 66 nm).

On the other hand, analyzing the SEM image at higher magnifications, (Fig. 2c) the average particle size of the nanoparticles within the fibers was calculated to be approximately 44 ± 7 nm (Fig. 3a). This result agrees with the theoretical estimation of the nanoparticle diameter obtained from the equation $NP_{size} = (0{,}78\ (\lambda_{LSPR})\text{-}266)$ nm [41],

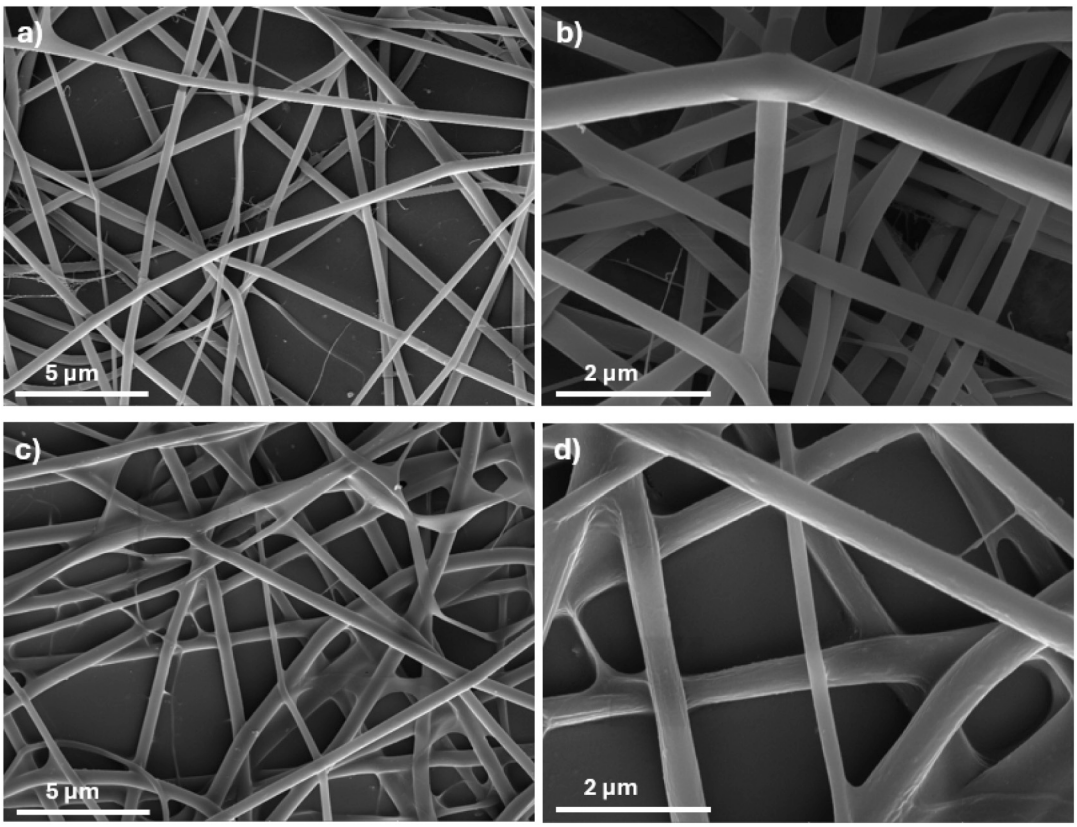


Fig. 1. SEM images of PVA fibers before (a,b) and after crosslinking (c,d).

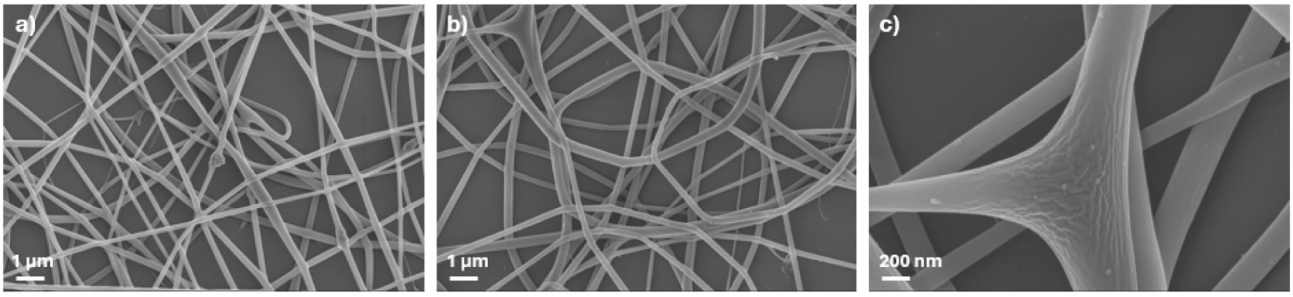


Fig. 2. FESEM images of a) AgNPs functionalized PVA fibers, b) AgNPs functionalized PVA fibers after crosslinking, c) a particular area with silver nanoparticles embedded into PVA nanofibers after crosslinking.

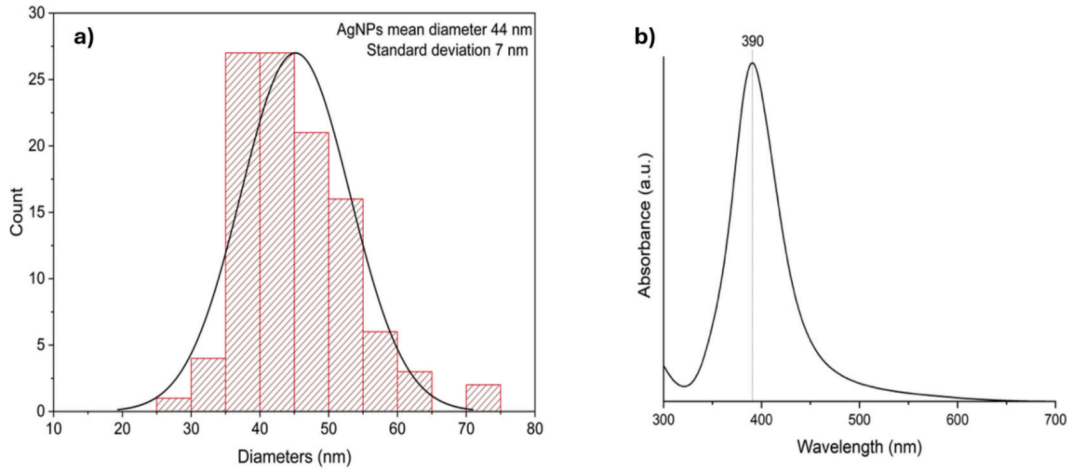


Fig. 3. a) Diameter distribution with relative mean diameter and standard deviation of AgNPs embedded in PVA nanofibers. b) UV–Vis spectrum of aqueous colloidal dispersion of silver nanoparticles.

which correlates the wavelength of the absorption peak of the plasmon (λ_{LSPR}) with the silver nanoparticle diameter (NP_{size}). The plasmon resonance peak was observed at 390 nm (Fig. 3b), with a resulting nanoparticle size of approximately 38 nm.

Regarding the second approach, FESEM images of the crosslinked uncoated and co-sputtered fibers are presented in Fig. 4. The sputtered fibers exhibit a uniform coating with the SiO_2Ag and ZrO_2Ag composite coatings, without compromising the nanostructure, a critical feature for electrospun membranes. No visible damage, such as changes in fiber shape or size, fiber fusion, collapse or pore occlusion, was observed. This indicates that the deposition conditions were appropriate for the nanostructured substrate. In fact, such damage can occur in PVD processes on small electrospun fibers [56]. These effects can depend on factors like the properties of the polymer substrate and the deposition process characteristics, which influence the energy of the depositing species and their impact on the coated fibers [46]. In this work, PVA fibers were successfully functionalized without causing significant damage, achieved by optimizing the deposition technique, process parameters, and deposition time. The addition of the coatings, either with silica or zirconia matrix, led in both cases to an increase in fibers diameter as shown in Table 1. A representative example of the coating thickness measurement procedure is provided in Fig. SI-2 for the PVA-SiO_2Ag sample and in Fig. SI-3 for the PVA-ZrO_2Ag sample; the full comparison of the diameter distributions of the PVA fibers before and after coating deposition is reported in Fig. SI-4.

The fibers were examined using EDS to compare the amount of silver introduced into the fibers and present in the coatings. The results are presented in Table 2. The amount of silver introduced during the electrospinning process, obtained by mixing the colloidal AgNPs solution with the polymer solution, varies depending on the polymer mass and electrospinning parameters. In fact, adding a conductive agent like silver can alter the final properties of the polymeric fibers [57]. Applying a PVD coating, however, offers more control over the amount of deposited silver, as it can be adjusted by modifying the power applied to the sputtering target. As shown in Table 2, the amount of silver in the coated fibers is higher and exhibits a lower standard deviation compared to the silver content obtained from the nanoparticles in the electrospun fibers. In contrast, blending the colloidal AgNPs solution with the PVA solution during electrospinning can lead to an uneven distribution of nanoparticles within the fibers [58].

3.2. Water contact angle

The contact angle measurements reported in Fig. 6 demonstrate that PVA fibers, after crosslinking, exhibit a water contact angle close to 90°, indicating low hydrophilicity. After the coating deposition, the contact angle increased to nearly 130° for both samples. Although zirconia coatings have previously been preferred for humid environments due to the high solubility of silica in water [27], the significant increase in contact angle may be attributed to the hierarchical structure of the coated nanofiber system as illustrated in Fig. 5 [59]. This effect cannot be ascribed solely to the intrinsic properties or roughness of the coating itself, as evidenced by the lower contact angle values measured for the same coatings deposited on flat silicon wafers (Fig. 6 (b,c)). This is supported by the RMS roughness measurements done on the fiber profile before and after coating deposition (Table SI-1 and Fig. SI-5). The RMS roughness of PVA fibers is 3.4 ± 0.8 nm while it increases to 9.5 ± 2.7 nm for PVA-SiO_2Ag fibers and 14.3 ± 3.6 nm for PVA-ZrO_2Ag fibers. This increase reflects enhanced surface nanostructurization due to the coatings. Moreover, these results indicate that the wettability is

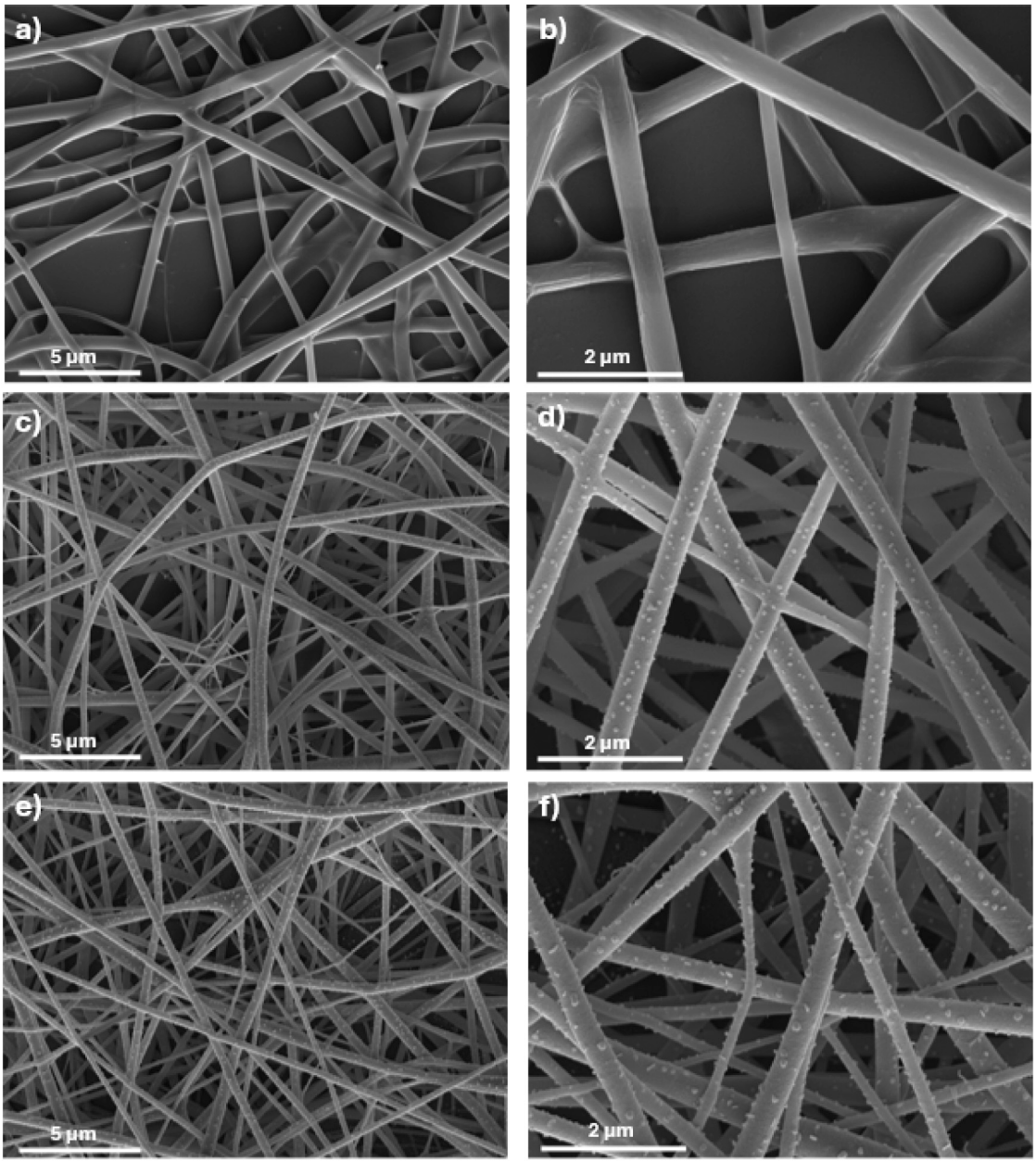


Fig. 4. FESEM images of crosslinked PVA (a,b), PVA- SiO_2Ag (c,d) and PVA- ZrO_2Ag (e,f) taken at different magnifications.

Table 1
Comparison between mean diameter and relative standard deviation of crosslinked fibers before and after coatings deposition and relative coatings thickness.

Sample	Mean diameter (nm)	Coating thickness (nm)
PVA	317 ± 104	–
PVA-SiO_2Ag	491 ± 90	87
PVA-ZrO_2Ag	390 ± 111	36.5

Table 2
Silver atomic percentage present in the samples.

	PVA-AgNPs	PVA-SiO_2Ag	PVA-ZrO_2Ag
Ag % at.	0.12 ± 0.05	1.28 ± 0.06	0.71 ± 0.06

governed by the combined contribution of the coating and the underlying fibrous morphology, rather than by the coating alone. This supports the potential of the coated fiber systems for use in filtration applications.

3.3. Leaching test in water

ICP–MS analysis enabled the quantification of silver in the PVA-AgNPs, PVA-SiO_2Ag, and PVA-ZrO_2Ag samples, and provided a benchmark for comparison with the values obtained from the silver ion release tests. The measured silver contents were 0.05 ± 0.01 ppm for PVA-AgNPs, 0.58 ± 0.01 ppm for PVA-SiO_2Ag, and 0.44 ± 0.07 ppm for PVA-ZrO_2Ag. Silver nanoparticles typically release silver ions when in contact with water or, in general, with aqueous solutions [60]. Generally, a higher concentration of ions in a solution corresponds to a greater number of silver nanoclusters. However, the presence of a composite coating with a matrix containing the antimicrobial agent can alter the release dynamics of it [36] depending on the properties of the matrix

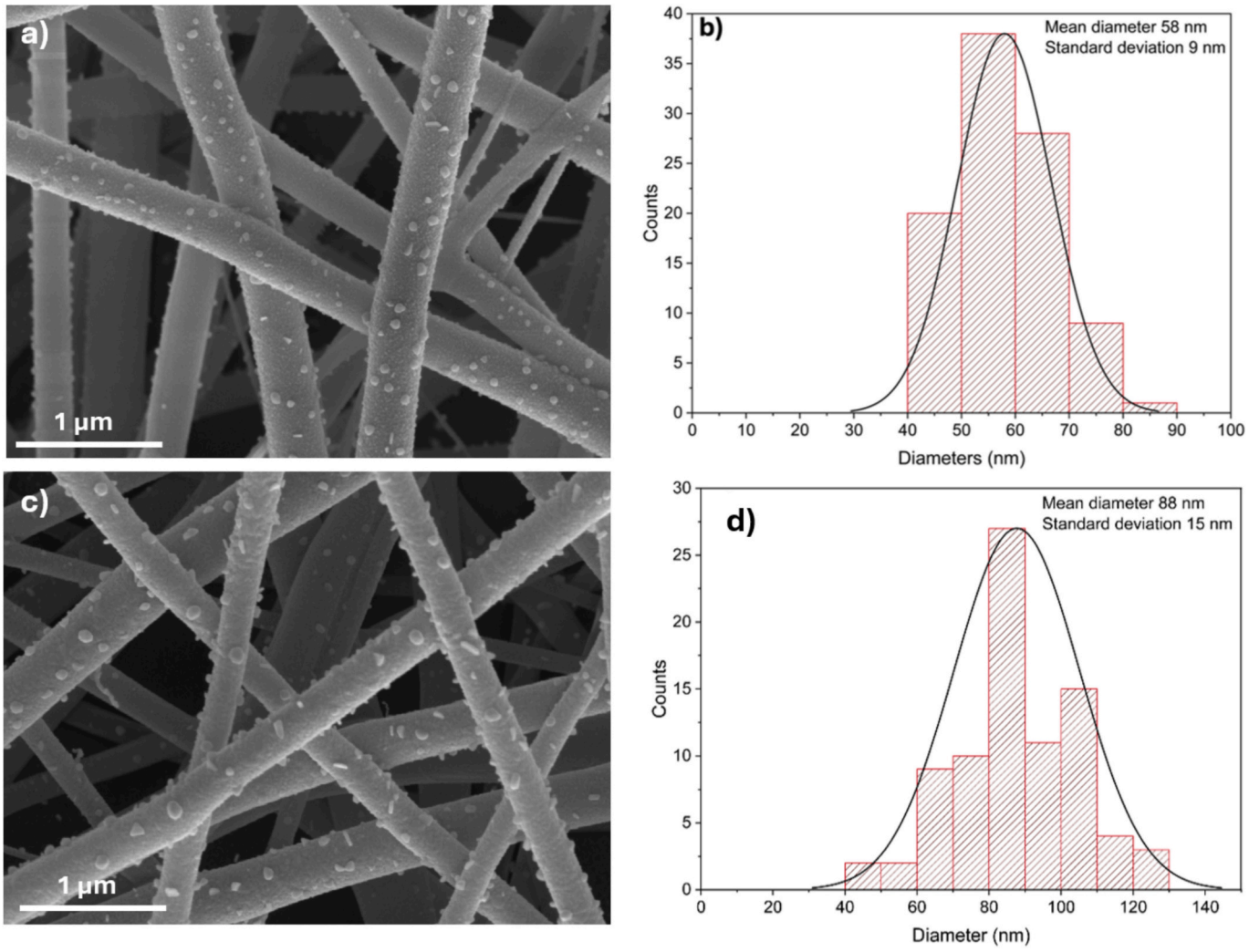


Fig. 5. FESEM images of PVA-SiO_2Ag coating (a) and with ZrO_2-Ag coating (c); diameter distribution of small particles on the surface of the crosslinked PVA fibers with SiO_2-Ag coating (b) and ZrO_2-Ag coating (d).

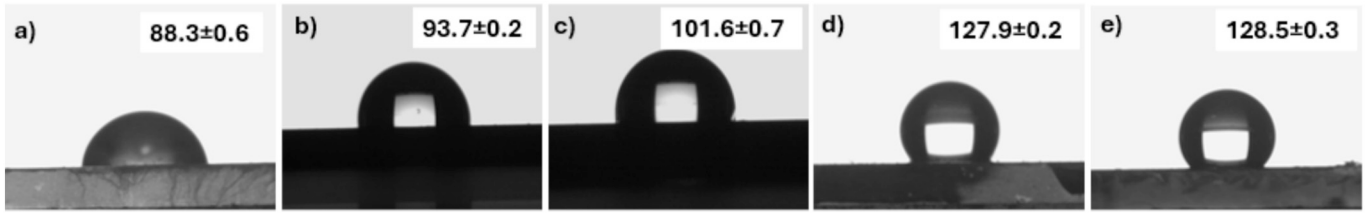


Fig. 6. Water contact angle of AgNPs functionalized PVA fibers (a), SiO_2Ag coating on silicon wafer (b), ZrO_2Ag coating on silicon wafer (c), PVA-SiO_2Ag (d) and PVA-ZrO_2Ag (e).

itself. For example, a matrix with higher solubility, like the SiO_2Ag coating, can influence ion release [27]. To investigate this, the silver ion release test was conducted in water on both co-sputtered coated and PVA-AgNPs membranes, comparing the effects of the two approaches over various immersion times. As shown in Fig. 7, the release profile of the coated fibers follows a typical logarithmic curve as commonly observed in coated samples [36] with the SiO_2Ag-coated fibers exhibiting the highest ion release. This behavior can be attributed both to the higher silver content in the coating, as confirmed by the EDS results in Table 2, and to the greater solubility in water of the SiO_2 matrix in water [27]. In contrast, the PVA-AgNPs sample shows no significant increase in silver ion release after the first three hours. This initial burst is likely due to the absence of a inorganic matrix, causing a rapid release within the first few hours of immersion, which is likely to happen in single-component decorated or porous fibers [61], as highlighted in Fig. 7b. The lack of a good fit to a double logarithmic model for the PVA-AgNPs sample over the entire experimental period suggests that the release kinetics are not consistent with a single diffusion-controlled mechanism. Instead, the deviation, particularly the abrupt release observed in the initial phase, indicates a burst release behavior followed by a slower release phase. Therefore, this sample shows poor control over silver release compared to the co-sputtered coated samples and is not suitable for long-term applications where sustained release is required. Comparison with ICP–MS results confirms that the PVA-AgNPs sample

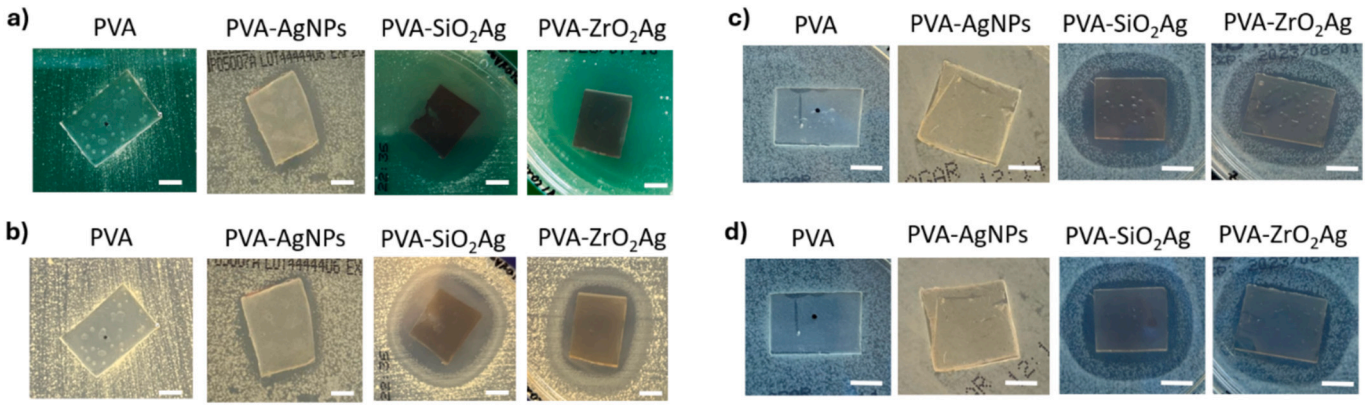


Fig. 7. Photographs of inhibition halo test against *S. epidermidis* relative to as spun PVA, AgNPs functionalized PVA, SiO_2-Ag and ZrO_2-Ag coated after 24h (a) and 48h(b) of incubation and *E. coli* (c,d) after 24h (c) and 48h(d) of incubation. Scale bars are 1 cm.

releases nearly all of its silver content within 14 days. The PVA-SiO₂Ag sample shows the highest release rate, with approximately 80 % of its silver released over the same period. The PVA-ZrO₂Ag sample exhibits a significantly slower release, with only about 47 % of the silver released after 14 days, which can be attributed to the lower solubility of the zirconia matrix in water compared to silica.

Additionally, the total amount of silver ions released over 14 days from the co-sputtered coated PVA membranes, is comparable to the amount released from coatings applied to cotton substrates with 1 h of deposition [27,36]. This is noteworthy, as a longer deposition time typically results in a thicker coating and, consequently, a higher silver content and greater ion release. In this case, the similar release levels suggest that the nanostructured morphology of the electrospun PVA fibers may promote more efficient silver ion release, possibly due to the higher surface area and enhanced coating-substrate interaction.

3.4. Antibacterial activity evaluation

To assess the antibacterial activity of the membranes, inhibition halo tests were carried out against *Staphylococcus epidermidis* and *Escherichia coli* (Fig. 8). After 24 and 48 h of incubation, distinct inhibition zones were observed around the PVA membranes functionalized with AgNPs and those coated via co-sputtering when tested against *S. epidermidis* (Fig. 8a, b). The inhibition zones measured approximately 1.5 cm in diameter for the functionalized membrane and 2.5 cm for the coated samples. Notably, after 48 h, a double inhibition zone appeared around the coated samples, consisting of a clear inner area completely free of bacterial growth, located near the membrane, and an outer, slightly darker zone where bacterial proliferation was slowed but not entirely inhibited. The total inhibition zone includes both regions. This phenomenon has been previously reported and confirmed in the literature [62].

In contrast, for *E. coli*, a more resistant Gram-negative bacterium [63], antibacterial activity was observed only in the co-sputtered coated samples (Fig. 8c, d), which showed an inhibition zone of approximately 2 cm in diameter. The PVA-AgNPs membranes did not exhibit any inhibition. This difference is likely due to the lower silver content in the functionalized membranes, as shown by EDS results in Table 2, and in their different release behavior reported in Fig. 8. The AgNPs embedded within the PVA fibers showed a rapid initial burst release followed by negligible further release, leading to insufficient and short-lived silver ion availability at the fiber surface; the total concentration of released silver ions was measured to be below the minimum inhibitory concentration (MIC) reported in the literature for several bacterial strains [64]. By contrast, the co-sputtered Physical vapor deposition (PVD)-coated samples provided a uniform surface distribution of silver nanoclusters and enabled a controlled, sustained release of silver ions, which likely supported their prolonged antibacterial activity. Interestingly, in the tests against *E. coli*, a double inhibition halo was already visible after only 24 h of incubation.

4. Conclusions

PVA membranes suitable for filtration applications were successfully electrospun, crosslinked, and modified using two different methods to confer antibacterial properties: one-pot synthesis of PVA-AgNPs with direct functionalization, and co-sputtering deposition of silver nanoclusters/silica or zirconia composite coatings. The fibers were morphologically characterized to assess any changes resulting from both processes. The comparative analysis of the two techniques indicates that

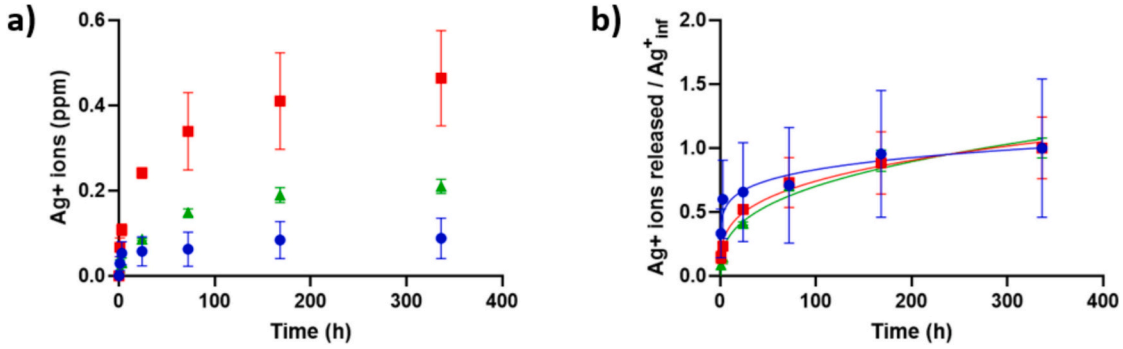


Fig. 8. a) The amount of ionic silver released in water during silver leaching test from functionalized samples (blue dots:PVA-AgNPs, red squares: PVA-SiO_2Ag, green triangles: PVA-ZrO_2Ag) along 14 days test (n = 3). b) Silver ions released normalized over the maximum quantity released at 14 days. A linear fit in double logaritmic scale is reported (R^2 = 0,49 for PVA-AgNPs – blue dots; R^2 = 0,89 for PVA-SiO_2Ag – red dots; R^2 = 0,96 for PVA-ZrO_2Ag – green triangles).

co-sputtered coating deposition is the most effective approach. This approach creates a hydrophobic hierarchical structure, allows for the controlled introduction of silver, ensures even distribution across the fiber surface, and provides efficient antibacterial properties. Additionally, the release characteristics are improved, with the matrix enhancing nanoparticle retention, thereby prolonging the antibacterial properties of the fibers.

CRediT authorship contribution statement

Francesca Gattucci: Writing – review & editing, Writing – original draft, Visualization, Investigation. **Martina Rossi:** Writing – review & editing, Writing – original draft, Visualization, Investigation. **Letizia Sarchini:** Investigation. **Chiara Bertarelli:** Writing – review & editing, Writing – original draft, Supervision, Resources, Funding acquisition. **Rossella Castagna:** Writing – review & editing, Writing – original draft, Visualization, Supervision, Methodology, Investigation. **Cristina Balagna:** Writing – review & editing, Writing – original draft, Resources, Project administration, Methodology, Funding acquisition, Conceptualization.

Declaration of competing interest

The authors declare that they have no known competing financial interests or personal relationships that could have appeared to influence the work reported in this paper.

Acknowledgments

This study was carried out within the MICS (Made in Italy – Circular and Sustainable) Extended Partnership and received funding from the European Union Next-GenerationEU (PIANO NAZIONALE DI RIPRESA E RESILIENZA (PNRR) – MISSIONE 4 COMPONENTE 2, INVESTIMENTO 1.3 – D.D. 1551.11-10-2022, PE00000004). This manuscript reflects only the authors' views and opinions, neither the European Union nor the European Commission can be considered responsible for them. Graphs and statistical analysis were done with GraphPad Prism 10 software.

Appendix A. Supplementary data

Supplementary data to this article can be found online at https://doi.org/10.1016/j.surfcoat.2025.133038.

Data availability

Data will be made available on request.

References

[1] A. Dhyani, T. Repetto, D. Bartikofsky, C. Mirabelli, Z. Gao, S.A. Snyder, C. Snyder, G. Mehta, C.E. Wobus, J.S. VanEpps, A. Tuteja, Surfaces with instant and persistent antimicrobial efficacy against bacteria and SARS-CoV-2, Matter 5 (2022) 4076–4091, https://doi.org/10.1016/j.matt.2022.08.018.
[2] S. Painuli, P. Semwal, R. Sharma, S. Akash, Superbugs or multidrug resistant microbes: a new threat to the society, Health Sci. Rep. 6 (2023) e1480, https://doi.org/10.1002/hsr2.1480.
[3] G. Moccia, O. Motta, C. Pironti, A. Proto, M. Capunzo, F. De Caro, An alternative approach for the decontamination of hospital settings, J. Infect. Public Health 13 (2020) 2038–2044, https://doi.org/10.1016/j.jiph.2020.09.020.
[4] O.V. Obayomi, D.C. Olawoyin, O. Oguntimehin, L.S. Mustapha, S.O. Kolade, P. O. Oladoye, S. Oh, K.S. Obayomi, Exploring emerging water treatment technologies for the removal of microbial pathogens, Curr. Res. Biotechnol. 8 (2024) 100252, https://doi.org/10.1016/j.crbiot.2024.100252.
[5] M. Rezaei, R.R. Netz, Airborne virus transmission via respiratory droplets: effects of droplet evaporation and sedimentation, Curr. Opin. Colloid Interface Sci. 55 (2021) 101471, https://doi.org/10.1016/j.cocis.2021.101471.
[6] Y. Nazarenko, C. Narayanan, P.A. Ariya, Indoor air purifiers in the fight against airborne pathogens: the advantage of circumferential outflow diffusers, Atmosphere 14 (2023) 1520, https://doi.org/10.3390/atmos14101520.
[7] E.S. Mousavi, N. Kananizadeh, R.A. Martinello, J.D. Sherman, COVID-19 outbreak and hospital air quality: a systematic review of evidence on air filtration and recirculation, Environ. Sci. Technol. 55 (2021) 4134–4147, https://doi.org/10.1021/acs.est.0c03247.
[8] P. Thangavel, D. Park, Y.-C. Lee, Recent insights into particulate matter (PM2.5)-mediated toxicity in humans: an overview, Int. J. Environ. Res. Public Health 19 (2022) 7511, https://doi.org/10.3390/ijerph19127511.
[9] R. Zomuansangi, C. Lalbiaktluangi, V.K. Gupta, A.A. Medders, J.E. Vidal, B. P. Singh, J.J. Song, P.K. Singh, A. Singh, B. Vellingiri, M. Iyer, M.K. Yadav, Interaction of bacteria and inhalable particulate matter in respiratory infectious diseases caused by bacteria, Atmos. Pollut. Res. 15 (2024) 102012, https://doi.org/10.1016/j.apr.2023.102012.
[10] M.-H. Yuan, S. Kang, K.-S. Cho, A review of phyto- and microbial-remediation of indoor volatile organic compounds, Chemosphere 359 (2024) 142120, https://doi.org/10.1016/j.chemosphere.2024.142120.
[11] K.M. Yun, C.J. Hogan, Y. Matsubayashi, M. Kawabe, F. Iskandar, K. Okuyama, Nanoparticle filtration by electrospun polymer fibers, Chem. Eng. Sci. 62 (2007) 4751–4759, https://doi.org/10.1016/j.ces.2007.06.007.
[12] J.T. Walker, A. Jhutty, S. Parks, C. Willis, V. Copley, J.F. Turton, P.N. Hoffman, A. M. Bennett, Investigation of healthcare-acquired infections associated with Pseudomonas aeruginosa biofilms in taps in neonatal units in Northern Ireland, J. Hosp. Infect. 86 (2014) 16–23, https://doi.org/10.1016/j.jhin.2013.10.003.
[13] H. Li, X. Chen, W. Lu, J. Wang, Y. Xu, Y. Guo, Application of electrospinning in antibacterial field, Nanomaterials 11 (2021) 1822, https://doi.org/10.3390/nano11071822.
[14] A. Greiner, J.H. Wendorff, Electrospinning: a fascinating method for the preparation of ultrathin fibers, Angew. Chem. Int. Ed. 46 (2007) 5670–5703, https://doi.org/10.1002/anie.200604646.
[15] S. Formenti, R. Castagna, R. Momentè, C. Bertarelli, F. Briatico-Vangosa, The relevance of extensional rheology on electrospinning: the polyamide/iron chloride case, Eur. Polym. J. 75 (2016) 46–55, https://doi.org/10.1016/j.eurpolymj.2015.12.003.
[16] J. Xue, T. Wu, Y. Dai, Y. Xia, Electrospinning and electrospun nanofibers: methods, materials, and applications, Chem. Rev. 119 (2019) 5298–5415, https://doi.org/10.1021/acs.chemrev.8b00593.
[17] B. Ding, M. Wang, J. Yu, G. Sun, Gas sensors based on electrospun nanofibers, Sensors 9 (2009) 1609–1624, https://doi.org/10.3390/s90301609.
[18] L. Hamui, M. Sánchez-Vergara, R. Sánchez-Ruiz, D. Ruanova-Ferreiro, R. Ballinas Indili, C. Álvarez-Toledano, New development of membrane base optoelectronic devices, Polymers 10 (2017) 16, https://doi.org/10.3390/polym10010016.
[19] R. Gopal, S. Kaur, Z. Ma, C. Chan, S. Ramakrishna, T. Matsuura, Electrospun nanofibrous filtration membrane, J. Membr. Sci. 281 (2006) 581–586, https://doi.org/10.1016/j.memsci.2006.04.026.
[20] R. Castagna, S. Donini, P. Colnago, A. Serafini, E. Parisini, C. Bertarelli, Biohybrid electrospun membrane for the filtration of Ketoprofen drug from water, ACS Omega 4 (2019) 13270–13278, https://doi.org/10.1021/acsomega.9b01442.
[21] R. Augustine, S.R.U. Rehman, R. Ahmed, A.A. Zahid, M. Sharifi, M. Falahati, A. Hasan, Electrospun chitosan membranes containing bioactive and therapeutic agents for enhanced wound healing, Int. J. Biol. Macromol. 156 (2020) 153–170, https://doi.org/10.1016/j.ijbiomac.2020.03.207.
[22] M. Blosi, A.L. Costa, S. Ortelli, F. Belosi, F. Ravegnani, A. Varesano, C. Tonetti, I. Zanoni, C. Vineis, Polyvinyl alcohol/silver electrospun nanofibers: biocidal filter media capturing virus-size particles, J. Appl. Polym. Sci. 138 (2021) 51380, https://doi.org/10.1002/app.51380.
[23] S.P. Deshmukh, S.M. Patil, S.B. Mullani, S.D. Delekar, Silver nanoparticles as an effective disinfectant: a review, Mater. Sci. Eng. C 97 (2019) 954–965, https://doi.org/10.1016/j.msec.2018.12.102.
[24] R. Castagna, R. Momentè, G. Pariani, G. Zerbi, A. Bianco, C. Bertarelli, Highly homogeneous core–sheath polyaniline nanofibers obtained by polymerisation on a wire-shaped template, Polym. Chem. 5 (2014) 6779–6788, https://doi.org/10.1039/C4PY00722K.
[25] P. Sagitha, C.R. Reshmi, S.P. Sundaran, A. Sujith, Recent advances in post-modification strategies of polymeric electrospun membranes, Eur. Polym. J. 105 (2018) 227–249, https://doi.org/10.1016/j.eurpolymj.2018.05.033.
[26] R. Erdem, M. İlhan, E. Sancak, Analysis of EMSE and mechanical properties of sputter coated electrospun nanofibers, Appl. Surf. Sci. 380 (2016) 326–330, https://doi.org/10.1016/j.apsusc.2015.11.204.
[27] A. Luceri, S. Perero, A. Cochis, A.C. Scalia, L. Rimondini, M. Ferraris, C. Balagna, Washing resistant antibacterial composite coatings on cotton textiles, Cellulose 30 (2023) 9877–9897, https://doi.org/10.1007/s10570-023-05471-7.
[28] Y. Yang, K. Kim, J. Ong, A review on calcium phosphate coatings produced using a sputtering process?An alternative to plasma spraying, Biomaterials 26 (2005) 327–337, https://doi.org/10.1016/j.biomaterials.2004.02.029.
[29] Q. Wei, Q. Li, D. Hou, Z. Yang, W. Gao, Surface characterization of functional nanostructures sputtered on fiber substrates, Surf. Coat. Technol. 201 (2006) 1821–1826, https://doi.org/10.1016/j.surfcoat.2006.03.007.
[30] N. Fiaschini, C. Giuliani, R. Vitali, L. Tammaro, D. Valerini, A. Rinaldi, Design and manufacturing of antibacterial electrospun polysulfone membranes functionalized by Ag nanocoating via magnetron sputtering, Nanomaterials 12 (2022) 3962, https://doi.org/10.3390/nano12223962.
[31] A.M. Manakhov, N.A. Sitnikova, A.R. Tsygankova, A.Yu. Alekseev, L.S. Adamenko, E. Permyakova, V.S. Baidyshev, Z.I. Popov, L. Blahová, M. Eliáš, L. Zajíčková, A. O. Solovieva, Electrospun biodegradable nanofibers coated homogenously by cu magnetron sputtering exhibit fast ion release. Computational and experimental study, Membranes 11 (2021) 965, https://doi.org/10.3390/membranes11120965.

[32] J.A.-D. Olmo, L. Ruiz-Rubio, L. Pérez-Alvarez, V. Sáez-Martínez, J.L. Vilas-Vilela, Antibacterial coatings for improving the performance of biomaterials, Coatings 10 (2020) 139, https://doi.org/10.3390/coatings10020139.
[33] M. Ferraris, S. Perero, M. Miola, S. Ferraris, G. Gautier, G. Maina, G. Fucale, E. Verne, Chemical, mechanical, and antibacterial properties of silver nanocluster–silica composite coatings obtained by sputtering, Adv. Eng. Mater. 12 (2010), https://doi.org/10.1002/adem.200980076.
[34] M. Ferraris, S. Perero, M. Miola, S. Ferraris, E. Verné, J. Morgiel, Silver nanocluster–silica composite coatings with antibacterial properties, Mater. Chem. Phys. 120 (2010) 123–126, https://doi.org/10.1016/j.matchemphys.2009.10.034.
[35] M. Ferraris, C. Balagna, S. Perero, Method for the Application of an Antiviral Coating to a Substrate and relative coating, WO2019/082001, 2019.
[36] M. Irfan, S. Perero, M. Miola, G. Maina, A. Ferri, M. Ferraris, C. Balagna, Antimicrobial functionalization of cotton fabric with silver nanoclusters/silica composite coating via RF co-sputtering technique, Cellulose 24 (2017) 2331–2345, https://doi.org/10.1007/s10570-017-1232-y.
[37] C. Balagna, S. Perero, E. Percivalle, E.V. Nepita, M. Ferraris, Virucidal effect against coronavirus SARS-CoV-2 of a silver nanocluster/silica composite sputtered coating, Open Ceram. 1 (2020) 100006, https://doi.org/10.1016/j.oceram.2020.100006.
[38] C. Balagna, R. Francese, S. Perero, D. Lembo, M. Ferraris, Nanostructured composite coating endowed with antiviral activity against human respiratory viruses deposited on fibre-based air filters, Surf. Coat. Technol. 409 (2021) 126873, https://doi.org/10.1016/j.surfcoat.2021.126873.
[39] A. Luceri, R. Francese, S. Perero, D. Lembo, M. Ferraris, C. Balagna, Antibacterial and antiviral activities of Silver nanocluster/silica composite coatings deposited onto air filters, ACS Appl. Mater. Interfaces 16 (2024) 3955–3965, https://doi.org/10.1021/acsami.3c13843.
[40] A. Shenava, Synthesis of silver nanoparticles by chemical reduction method and their antifungal activity, Int. Res. J. Pharm. 4 (2013) 111–113, https://doi.org/10.7897/2230-8407.041024.
[41] S. Chernousova, M. Epple, Silver as antibacterial agent: ion, nanoparticle, and metal, Angew. Chem. Int. Ed. 52 (2013) 1636–1653, https://doi.org/10.1002/anie.201205923.
[42] J.L. Clement, P.S. Jarrett, Antibacterial silver, Metal-Based Drugs 1 (1994) 467–482, https://doi.org/10.1155/MBD.1994.467.
[43] W.-C. Chen, C.-Y. Ko, K.-C. Chang, C.-H. Chen, Influences of processing and sterilizing strategies on reduced silver nanoparticles in poly(vinyl alcohol) electrospun membranes: optimization and preservation of antibacterial activity, Mater. Chem. Phys. 254 (2020) 123300, https://doi.org/10.1016/j.matchemphys.2020.123300.
[44] Z. Zhang, Y. Wu, Z. Wang, X. Zou, Y. Zhao, L. Sun, Fabrication of silver nanoparticles embedded into polyvinyl alcohol (Ag/PVA) composite nanofibrous films through electrospinning for antibacterial and surface-enhanced Raman scattering (SERS) activities, Mater. Sci. Eng. C 69 (2016) 462–469, https://doi.org/10.1016/j.msec.2016.07.015.
[45] H. Kadavil, M. Zagho, A. Elzatahry, T. Altahtamouni, Sputtering of electrospun polymer-based nanofibers for biomedical applications: a perspective, Nanomaterials 9 (2019) 77, https://doi.org/10.3390/nano9010077.
[46] D. Valerini, L. Tammaro, R. Vitali, G. Guillot, A. Rinaldi, Sputter-deposited Ag nanoparticles on electrospun PCL scaffolds: morphology, wettability and antibacterial activity, Coatings 11 (2021) 345, https://doi.org/10.3390/coatings11030345.
[47] I. Maliszewska, T. Czapka, Electrospun polymer nanofibers with antimicrobial activity, Polymers 14 (2022) 1661, https://doi.org/10.3390/polym14091661.
[48] Y. Meng, A sustainable approach to fabricating ag nanoparticles/PVA hybrid nanofiber and its catalytic activity, Nanomaterials 5 (2015) 1124–1135, https://doi.org/10.3390/nano5021124.
[49] H.K. Lee, E.H. Jeong, C.K. Baek, J.H. Youk, One-step preparation of ultrafine poly (acrylonitrile) fibers containing silver nanoparticles, Mater. Lett. 59 (2005) 2977–2980, https://doi.org/10.1016/j.matlet.2005.05.005.
[50] C. Balagna, S. Perero, F. Bosco, C. Mollea, M. Irfan, M. Ferraris, Antipathogen nanostructured coating for air filters, Appl. Surf. Sci. 508 (2020) 145283, https://doi.org/10.1016/j.apsusc.2020.145283.
[51] C. Balagna, M. Irfan, S. Perero, M. Miola, G. Maina, D. Santella, A. Simone, Characterization of antibacterial silver nanocluster/silica composite coating on high performance Kevlar® textile, Surf. Coat. Technol. 321 (2017) 438–447, https://doi.org/10.1016/j.surfcoat.2017.05.009.
[52] C. Balagna, M. Irfan, S. Perero, M. Miola, G. Maina, M. Crosera, D. Santella, A. Simone, M. Ferraris, Antibacterial nanostructured composite coating on high performance Vectran™ fabric for aerospace structures, Surf. Coat. Technol. 373 (2019) 47–55, https://doi.org/10.1016/j.surfcoat.2019.05.076.
[53] NCCLS M2-A9, Performance Standards for Antimicrobial Disk Susceptibility Tests, Approved Standard, 9th ed., NCCLS, Villanova, PA, 2003 (n.d.).
[54] J.Y. Cheon, Y.O. Kang, W.H. Park, Formation of ag nanoparticles in PVA solution and catalytic activity of their electrospun PVA nanofibers, Fibers Polym. 16 (2015) 840–849, https://doi.org/10.1007/s12221-015-0840-0.
[56] G. Pagnotta, G. Graziani, N. Baldini, A. Maso, M.L. Focarete, M. Berni, F. Biscarini, M. Bianchi, C. Gualandi, Nanodecoration of electrospun polymeric fibers with nanostructured silver coatings by ionized jet deposition for antibacterial tissues, Mater. Sci. Eng. C 113 (2020) 110998, https://doi.org/10.1016/j.msec.2020.110998.
[57] Y. Gao, Y. Bach Truong, Y. Zhu, I. Louis Kyratzis, Electrospun antibacterial nanofibers: production, activity, and *in vivo* applications, J. Appl. Polym. Sci. 131 (2014) app.40797, https://doi.org/10.1002/app.40797.
[58] O. Velgosova, L. Mačák, E. Múdra, M. Vojtko, M. Lisnichuk, Preparation, structure, and properties of PVA–AgNPs nanocomposites, Polymers 15 (2023) 379, https://doi.org/10.3390/polym15020379.
[59] N. Zander, Hierarchically structured electrospun fibers, Polymers 5 (2013) 19–44, https://doi.org/10.3390/polym5010019.
[60] B. Tomšič, B. Simončič, B. Orel, L. Černe, P.F. Tavčer, M. Zorko, I. Jerman, A. Vilčnik, J. Kovač, Sol–gel coating of cellulose fibres with antimicrobial and repellent properties, J. Sol-Gel Sci. Technol. 47 (2008) 44–57, https://doi.org/10.1007/s10971-008-1732-1.
[61] M.M. Asli, B. Pourdeyhimi, E.G. Loboa, Release profiles of tricalcium phosphate nanoparticles from poly(L -lactic acid) electrospun scaffolds with single component, core–sheath, or porous fiber morphologies: effects on hASC viability and osteogenic differentiation, Macromol. Biosci. 12 (2012) 893–900, https://doi.org/10.1002/mabi.201100470.
[62] C. Mollea, F. Bosco, D. Fissore, Agar plate methods for assessing the antibacterial activity of thyme and oregano essential oils against *S. epidermidis* and *E. coli*, Antibiotics 11 (2022) 1809, https://doi.org/10.3390/antibiotics11121809.
[63] J.L. Graves, M. Tajkarimi, Q. Cunningham, A. Campbell, H. Nonga, S.H. Harrison, J.E. Barrick, Rapid evolution of silver nanoparticle resistance in Escherichia coli, Front. Genet. 6 (2015), https://doi.org/10.3389/fgene.2015.00042.
[64] L. Kvitek, A. Panacek, R. Prucek, J. Soukupova, M. Vanickova, M. Kolar, R. Zboril, Antibacterial activity and toxicity of silver – nanosilver versus ionic silver, J. Phys. Conf. Ser. 304 (2011) 012029, https://doi.org/10.1088/1742-6596/304/1/012029.